

## DEVELOPMENT OF A CLIMATOLOGY OF CLOUD PROPERTIES DERIVED FROM GOES OVER THE SOUTHEASTERN PACIFIC FOR PACS

J. Kirk Ayers\*

Analytical Services & Materials Inc., Hampton, VA

Patrick Minnis, David F. Young, William L. Smith, Jr., and Louis Nguyen  
Atmospheric Sciences, NASA-Langley Research Center, Hampton, VA

### 1. INTRODUCTION

A goal of the NOAA Pan American Climate Studies (PACS) Program is to understand the role of the trade winds, sea surface temperature, and the subtropical stratocumulus systems, especially over the southeastern Pacific (SEP), in the maintenance and variability of the eastern Pacific intertropical convergence zone (ITCZ). Determination of the cloud properties and their interaction with the radiation budget and SST are crucial to understanding the relationship between the subtropical highs and the deep convection over the eastern Pacific. This paper presents the results of an initial analysis of 3-hourly multispectral GOES-8 data to derive cloud macrophysical and microphysical properties as well as the radiation budget over the SEP and adjacent continental areas. Cloud amount, height, phase, effective particle size, optical depth, and liquid/ice water path are derived along with shortwave SW albedo, and the top-of-atmosphere (TOA) longwave flux on a 1.0° latitude-longitude grid for a domain encompassed by 20°N, 40°S, 60°W, and 115°W, shown in Fig. 1. The initial analyses focus on the period between October and November 1999 when research ships from Chile and the USA were operating in the domain. Data from radar and a ceilometer aboard the ships are used to validate the retrievals from GOES-8. These analyses are the first steps in the process of developing climatologies of cloud and radiation properties for use in meso- and large-scale models of the circulation in the southeastern Pacific.

### 2. METHODOLOGY

This study utilizes the Visible Infrared Solar-Infrared Split Window Technique (VISST) to determine cloud properties. VISST is a 4-channel model-matching method for plane parallel clouds. It is discussed further by Minnis et al. (2001). VISST requires 4-km pixel resolution GOES-8 satellite images and uses the following channels: 0.65  $\mu\text{m}$  (VIS), 3.9  $\mu\text{m}$  (SIR), 10.8  $\mu\text{m}$  (IR), and 12.0  $\mu\text{m}$  (SWC). The GOES-8 data for each channel were calibrated by Minnis et al. (2001) using coincident data from the Visible Infrared Radiometer (VIRS) on the Tropical Rainfall Measuring Mission

---

\* *Corresponding Author Address:* J. K. Ayers, AS&M, Inc., 1 Enterprise Parkway Hampton, VA 23666; E-mail: j.k.ayers@larc.nasa.gov.

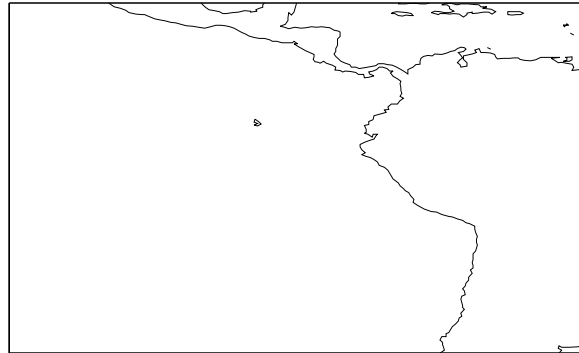


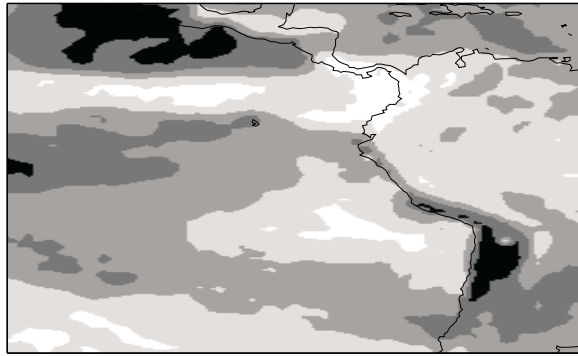
Figure 1. Analysis domain.

satellite (TRMM). No changes were made to the nominal GOES-8 SIR, IR, and SWC data.

Several additional inputs are required to facilitate satellite retrievals. Atmospheric profiles (1° resolution) derived from ECMWF 6-hourly model runs are used for skin temperature, cloud height calculation, and humidity profiles. Surface type is based on the IGBP 10-minute resolution surface map, remapped to an albedo representation. Clear-sky reflectances, and ice and snow masks developed for the Clouds and the Earth's Radiant Energy System (CERES) program are used for additional surface characterization (Trepte et al. 1999). Narrowband-to-broadband flux conversion functions, developed from correlations of coincident ERBE-scanner broadband and GOES narrowband fluxes are used to compute broadband shortwave and longwave fluxes from the GOES data.

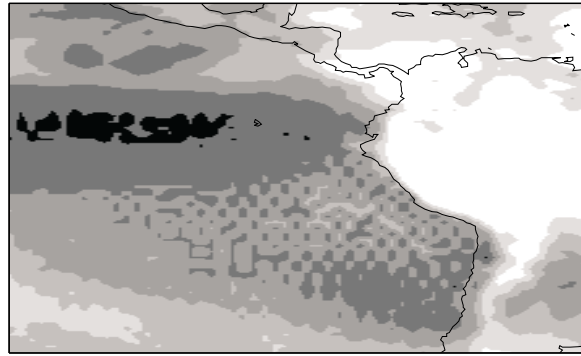
### 3. MONTHLY SUMMARIES

Several examples of monthly mean cloud products for November 1999 are shown in Figs. 2 - 7. Mean cloud coverage and cloud-top heights for the month are shown in Figs. 2 and 3, respectively. The areas of deep convection, identified by mean cloud heights over 5 km, are primarily located over South and Central America. The ITCZ over the Pacific is apparent in the elevated cloud amounts near 10°N, but deep convection is not as frequent there as over Central America because the mean cloud heights do not exceed 4 km. Nevertheless, the northern part of the ITCZ where cloud tops are higher is probably a region where rainfall occurs. The smallest cloud amounts are found over the Atacama Desert while the greatest cloud amounts are found over the



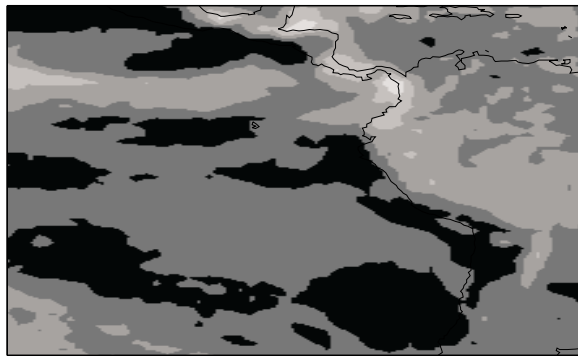
0 20 40 60 80 100  
Cloud Fraction (%)

Fig. 2. November 1999 mean cloud fraction.



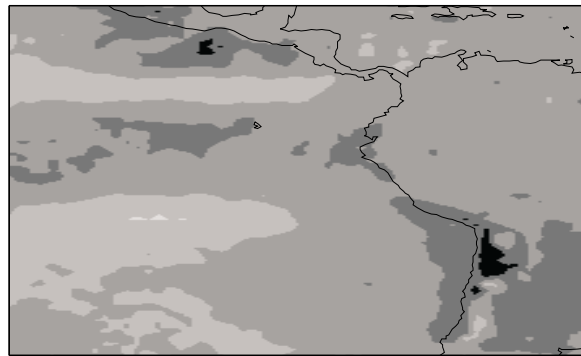
0 1 2 3 4 5 5+  
Cloud Height (km)

Fig. 3. November 1999 mean cloud-top height.



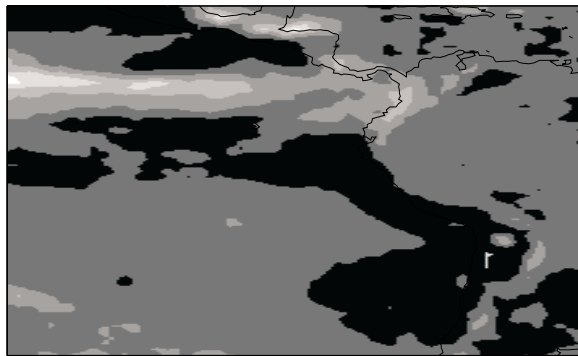
0 12 24 36  
Optical Depth

Fig. 4. November 1999 mean optical depth.



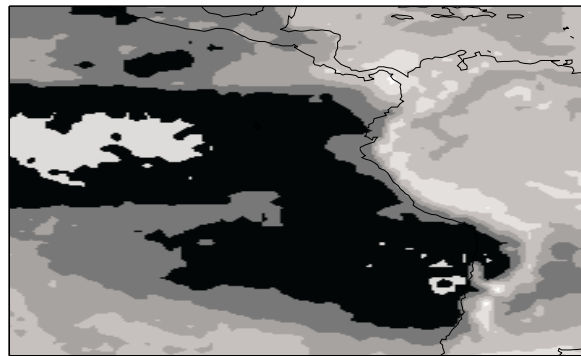
0 10 20 30  
Droplet Radius (um)

Fig. 5. November 1999 mean water droplet radius.



0 100 200 300  
Liquid Water Path (g/m2)

Fig. 6. November 1999 mean liquid water path.



0 20 40 60  
Effective Diameter (um)

Fig. 7. November 1999 mean ice crystal effective diameter.

Amazon Basin and the stratocumulus region off the western coast of Chile. Increased cloud fraction over the Southern Hemispheric storm track is visible in the southernmost portion of the figure. Cloud tops are lowest just south of the ITCZ and near the Chilean coast. The mottled pattern in Fig. 3 over the ocean is an

artifact of the gridded soundings and SSTs used in the analysis.

Mean optical depth  $\tau$ , shown in Fig. 4, varies from 3 over some ocean areas to nearly 35 over Panama. The heavier cloud cover in the ITCZ has relatively larger values of  $\tau$ . The SEP stratocumulus region shows  $\tau$

decreasing around its edges. The mean water droplet radius  $r_e$  distribution for the analysis domain in Fig. 5 reveals smaller droplets near the Mexican and Chilean coasts and also south of the ITCZ. The smaller effective radii over the SEP tend to follow the cold current into the ITCZ. Larger droplets are found over the Amazon Basin, the ITCZ, and in the western part of the SEP stratocumulus region. The mean  $r_e$  for the ITCZ is in the 15 to 20  $\mu\text{m}$  range, which is usually associated with precipitation. The westward increase in  $r_e$  from the Chilean coast was also observed during October 1999 from GOES-8 (Garreaud et al. 2001).

The mean liquid water path  $LWP$  for the domain in Fig. 6 shows values ranging from 150 to 300  $\text{gm}^{-2}$  over the ITCZ. The smallest values are found along the cold current and north of the ITCZ as a result of the small values of  $r_e$  and  $\tau$  for the region.

The mean ice crystal effective diameters  $D_e$  are shown in Fig. 7. The light gray region near the center of the western edge of the domain is an area where no ice retrievals were found. Many of the small values of  $D_e$  over the SEP are probably underestimated because most of the retrievals were affected by the low clouds underneath the thin cirrus. The ice particle sizes over the Andes and the ITCZ are more accurate and larger because the clouds are optically thick and the 3.9- $\mu\text{m}$  radiance is unaffected by the lower clouds. Examination of individual scenes reveals larger ice crystals for thin cirrus over an otherwise cloud-free ocean. The mean ice water path  $IWP$  (not shown) varies from 0 to over 300  $\text{gm}^{-2}$ ; the largest values are found over the areas of deep convection. The percentage of the observed clouds that were identified as ice clouds is shown in Fig. 8. More than half of the cloudiness over the entire Amazon Basin and Caribbean Sea is composed of ice. A smaller percentage of ice occurs over the ITCZ while very few ice clouds were observed over the SEP stratocumulus area (black in the figure).

#### 4. VALIDATION

During November 1999 the NOAA *R/V Ron Brown* cruised the region, 8°N - 8°S, 95°W - 110°W, collecting a wide range of meteorological and oceanographic data, (<http://www.ogp.noaa.gov/mpe/clivar/pacs/fy99/fairall/fairall99.htm>). Data from the ceilometer, cloud radar, and microwave radiometer aboard the *Ron Brown* are used for assessing the satellite retrievals. The validation is effected by comparing VISST cloud properties averaged for a 0.5° box centered on the ship with half-hourly means from the ship data. Cloud amount is computed from the ceilometer data by dividing the number of cloud returns by the total number of shots. Cloud-top height is derived from the radar data and the  $LWP$  is computed from the microwave radiometer measurements.

##### Cloud Fraction

Overall the mean cloud fraction from VISST is 36.8% compared to 39.7% from the ceilometer. The standard

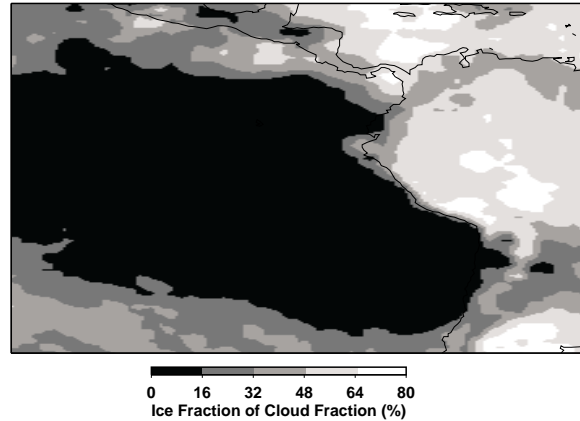


Fig. 8. Percentage of observed cloud amount classified as ice cloud.

deviation of the differences is 19%. The cloud amounts are in good agreement when the cloud fraction is either less than 20% or greater than 80% (Table 1). The approximately 30% of the time when the agreement is poor can be attributed to several factors. In a few cases, the column directly over the Brown was clear but, from the satellite imagery, clouds were obviously present in the box. Mid and high level clouds, which can be observed by satellite but not by the ceilometer, could contribute to the scatter. Those cloud types may account for the VISST values in the 40-60% range for the nearly clear ship observations,

##### Cloud Height

The VISST and radar cloud-top heights are compared in Fig. 9. The non-filled circles are a direct comparison of all coincident data. The resulting curve fit shows that the radar measurements are somewhat higher than those from VISST for  $z_c < 1.5$  km, but the agreement is better for higher clouds. Overall,  $z_c(\text{GOES})$  is  $0.15 \pm 0.55$  km lower than  $z_c(\text{radar})$ . This level of agreement is similar to that found over the southeastern Pacific by Garreaud et al. (2001) for a comparison of GOES-8 data analyzed with VISST over the southeastern Pacific during October 1999. The largest contributors to the difference here are multi-level clouds and multiple inversions. If only single layer clouds are considered (filled circles), the agreement is even better.

##### Liquid Water Path

VISST-derived and ship microwave  $LWP$  amounts are compared in Fig. 10. The two datasets are reasonably well correlated but appear to have an offset. The mean microwave  $LWP$  is 87.2  $\text{gm}^{-2}$  which is 13.5  $\text{gm}^{-2}$  greater than the VISST average. These results were obtained using a global baseline of 10  $\text{gm}^{-2}$  for the microwave data. Work is in progress to correct a diurnal cycling problem and to adjust the baseline of the microwave  $LWP$  retrievals (C. F. Fairall, personal communication). New  $LWP$  values might improve the correlation.

Table 1. Comparison of *R/V Ron Brown* ceilometer and VISST cloud fractions.

R. Brown	VISST				
	0-20	20-40	40-60	60-80	80-100
0-20	19	1	5	0	0
20-40	4	1	1	0	0
40-60	0	0	1	0	0
60-80	0	0	1	0	0
80-100	0	1	1	1	12

## 5. CONCLUDING REMARKS

The SEP contains a variety of interesting features that should be reproduced in climate or regional forecast models. For example, variations in cloud particle size may be correlated with SST, the intensity of the subtropical high, or the availability of cloud condensation nuclei. Significant changes in cloud amount, optical depth, and *LWP* occur as a function of local time (not shown). Thus, the relatively static picture presented here does not capture one of the main features of clouds in this part of the world. Such characteristics should be taken into account when modeling the atmosphere in this area.

The initial validations from this study indicate that the VISST method applied to GOES data can produce reliable cloud macrophysical and microphysical properties over the PACS region. The ship observations will be refined further to obtain final validation for this particular cruise. Additional study using ship observations from other *R/V Ron Brown* cruises in the same area will be analyzed to improve the statistical reliability of the validations and to better understand the retrievals. Concurrently, the GOES-8 data will be analyzed continuously for a long time period beginning in 1996 to determine the differences in the SEP cloud features during and after El Ninos.

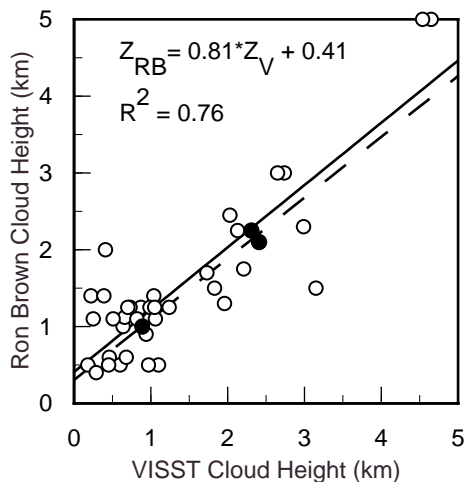


Fig. 9. Comparison of radar and VISST cloud heights.

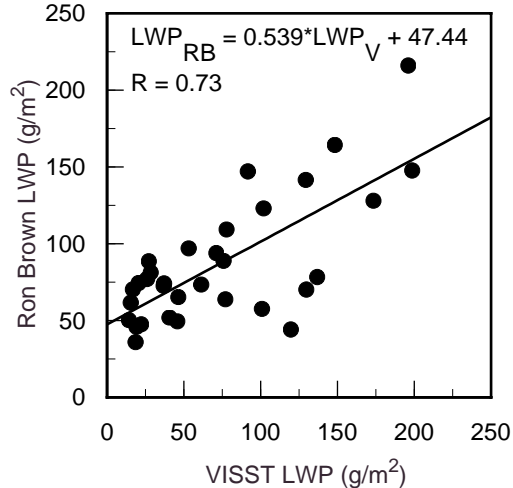


Fig. 10. Comparison of VISST and microwave LWP.

## Acknowledgments

This work was supported by the NOAA PACS Program under NOAA agreement NA00AANRG0330. Many thanks to Dr. Chris Fairall for providing the preliminary data from the *R/V Ron Brown*, and to Pat Heck, Anita Rapp, Mandana Khaiyer, and David Doelling for helping to implement the satellite analysis programs. The atmospheric profiles were generated by the CERES Meteorological, Ozone, and Aerosols group and obtained from the NASA Langley Atmospheric Sciences Data Center.

## References

- Garreaud, R. D., J. Rutllant, J. Quintana, J. Carrasco, and P. Minnis, 2001: CIMAR-5: A snapshot of the lower troposphere over the subtropical southeast Pacific. *Bull. Amer. Meteorol. Soc.*, October issue.
- Minnis, P., L. Nguyen, D. F. Young, D. R. Doelling and W. F. Miller, 2001: Rapid calibration of Operational and research meteorological satellite imagers, Part I: Use of the TRMM VIRS or ERS-2 ATSR-2 as a reference. Submitted to *J. Atmos. Oceanic Technol.*
- Minnis, P., et al., 2001: A near-real time method for deriving cloud and radiation properties from satellites for wether and climate studies. *Proc. AMS 11<sup>th</sup> Conf. Satellite Meteor. and Oceanogr.*, Madison, WI, October 15-18.
- Trepte, Q., Y. Chen, S. Sun-Mack, P. Minnis, D. F. Young, B. A. Baum, and P. W. Heck, 1999: Scene identification for the CERES cloud analysis subsystem. *Proc. AMS 10<sup>th</sup> Conf. Atmos. Rad.*, Madison, WI, June 28 – July 2, 1999, 169-172.